



Transformer Fault Location Classification Using FFT Based 1D-Convolutional Neural Network Model

Priyanka Tiwari^{1*}, Shweta Singh², Naresh Bangari³

^{1,2} Department of Electrical Engineering, Maharishi University, Lucknow, UP, India.

³ Department of Electrical Engineering, DU, Dinjan, Assam, India.

Citation: Priyanka Tiwari, et.al (2024), Transformer Fault Location Classification Using FFT Based 1D-Convolutional Neural Network Model, *Educational Administration: Theory and Practice*, 30(5), 4148- 4156
Doi: 10.53555/kuey.v30i5.3596

ABSTRACT

Vibration signals serve as indicators of an electrical device's condition, comprising multiple harmonics that elucidate its operational state. Analyzing the harmonic frequency and magnitude within the vibration signal enables the identification of fault locations in the machine or device. This work proposes the use of a fault location classification based on Fast Fourier Transform (FFT) for feature extraction and an 1D Convolutional neural network model to distinguish the difference between 3 types of deformation conditions that were collected from transformer surface. The vibration sensor data in the time-series domain, thus the primary reason for the development of 1D-CNNs. A reduction in the amount of computational work that the network needs to do is made possible by the proposed 1D-CNN model. The primary objective is to analyze vibration signals of the transformer core in order to diagnose fault location, with the data being measured in the time domain. With a classification accuracy of 96.6%, the CNN model that was created for the purpose of detecting faults in transformer cores displayed an amazing performance.

1. INTRODUCTION

The Power transformers play a crucial role in ensuring reliable power delivery within the power system and a key component responsible for voltage conversion, power distribution, and transmission. In the event of transformer failure, there is a high likelihood of large-scale blackouts, leading to significant direct and indirect economic losses[1],[2]. To minimize the incidence of unexpected failures, various diagnostic and monitoring techniques have been developed. According to recent studies, transformer failures can be categorized into three types: electrical, mechanical, and thermal defects. Thus, early detection of faults and evaluation of the health status of power transformers are essential. The use of vibration signals for assessing transformer health is a relatively new technique compared to other transformer condition monitoring methods, and research in this area is still in its early stages [3],[4]. As a non-intrusive online approach, vibration-based methods are suitable for evaluating the condition of power transformers.

A vibration sensor is utilized in the process of vibration analysis in order to measure the vibration signal that is produced by the core components. For the purpose of facilitating online condition monitoring of the transformer, time-frequency domain characteristics are retrieved.

Techniques that fall under the heading of external detection and analysis methods [5]-[7] include this particular method. However, despite these benefits, there are still substantial limits in monitoring winding and iron core problems. This is because there is a lack of in-depth study on the vibration characteristics of these components, as well as a lack of experience in this field.

Over the course of the last few years, convolutional neural networks, also known as CNNs, have shown a great deal of success in the field of pattern recognition[8]. CNNs are well-known for their capacity to independently extract features from signals or images. It is common practice for these networks to be constructed using two-dimensional convolutional neural networks, also known as 2D CNNs. Several Researchers proposed different CNN-based neural networks models for classification. The adoption of Deep Learning (DL) techniques has been shown in recent research to be a viable solution to the problem of skill dependency [9].

Compared to other models like Deep Belief Network [10],[11] Stacked Auto-encoder [12],[13] Recurrent Neural Network [14], and Long short-term memory [15], convolutional neural networks (CNNs) leverage local receptive fields, weight sharing, and spatial subsampling. These characteristics help reduce computational complexity and mitigate overfitting, thus enhancing pattern recognition accuracy and

efficiency. In the context of rolling bearing fault identification, CNNs are typically employed in two ways. Firstly, the original one-dimensional vibration signal can serve as the input to the model. Alternatively, the signal can be transformed into a two-dimensional image representation for input.

This paper outlines an analytical methodology for constructing a 1D CNN model designed for fault location identification in transformer core. The model is based on analyzing vibration modes that indicate the bending of limbs in the out-of-plane direction. Multiple experimental studies are under taken to simulate diverse critical faults in transformer operational conditions. The vibrational data recorded from these experiments with different load conditions are then analyzed using CNN models.

2. METHODOLOGY

2.1 Concept of vibration

The interaction of two phenomena is the primary cause of core vibration. These two phenomena are as follows: (i) winding vibration, which is caused by the electromagnetic force generated by the interaction of the current in a winding with leakage flux; and (ii) magnetostriction in the silicon steel sheet and the Maxwell electromagnetic force [16]-[19].

There are dimensional changes that take place in the silicon steel sheet as a result of the application of an external magnetic field. These changes include contraction and elongation. Following the removal of the magnetic field, the sheet will return to the dimensions that it had when it was first created. The magnetostrictive effect is the name given to this particular occurrence. There has been a considerable improvement in the overall control over transformer core vibration as a result of the developments in lamination processes for making the iron core and the employment of weft-free adhesive tape for binding. The magnetostriction of the silicon steel sheet has been the most important component in this improvement. It is usual practice to employ the magnetostriction ratio to reflect magnetostriction, which can be represented as equation (1).

$$\delta = \frac{\Delta L}{L} \quad (1)$$

Where δ is the silicon steel sheet axial magnetostriction ratio, ΔL is the silicon steel sheet maximum axial expansion or contraction, and L is the silicon steel sheet original axial dimension. Assuming the supply voltage is $V_1 = V_s \sin \omega t$, according to the principle of electromagnetic induction, the magnetic induction intensity in the core is

$$B = \frac{\phi}{A} = \frac{V_s}{\omega N A} \cos \omega t = A_0 \cos \omega t \quad (2)$$

Where ϕ is the core magnetic flux, A is the core cross sectional area, The magnetic field strength in the iron core is

$$H = \frac{B}{\mu} = B \frac{H_c}{B_s} = B_0 H_c \frac{\cos \omega t}{B_s} \quad (3)$$

A small-scale deformation of the SSS caused by magnetostriction satisfies the following relationship:

$$\frac{\nabla L}{L} \frac{1}{dH} = |H| \frac{2\varepsilon_s}{H_c^2} \quad (4)$$

Where ε_s is the saturation magnetostriction ratio of the silicon steel sheet. Based on the above relationship, one can derive the maximum axial elongation of the core caused by the silicon steel sheet magnetostriction as follows:

$$\nabla L = L \int_0^H |H| \frac{2\varepsilon_s}{H_c^2} dH = L \frac{\varepsilon_s H^2}{H_c^2} = \frac{L \varepsilon_s^2 V_s^2}{(\omega N_{core} B_s)^2} \cos^2 \omega t \quad (5)$$

In comparison to the alternating electromagnetic field, the variation period of magnetostriction is twice as long as the alternating electromagnetic field. On the other hand, the fundamental frequency of the core vibration that is induced by magnetostriction is twice as high as the variation frequency of the electromagnetic field, denoted by ω .

2.2 Problem formulation

Training datasets are often segmented into smaller portions, necessitating running algorithms on each fragment for predictions. This process can be time-consuming, thus to overcome this FFT optimization, we're streamlining these computations, reducing overall training time[20]. To enhance real-time analysis, we're integrating FFT algorithms to replace the conventional forward Convolution propagation in our models. The Fast Fourier Transform (FFT) algorithm is a fast computational method for efficiently computing the discrete-time signals, enabling rapid processing of signals in real-time applications. This optimization significantly accelerates processing for frameworks like YOLO[21], R-CNN [22], and Faster R-CNN [23], crucial for rapid decision-making.

2.3 Proposed methodology

The methodology entails assembling fault classification datasets and enhancing feature extraction using FFT to expedite diagnosis while enhancing accuracy. CNNs are then employed for the training and testing phases of fault diagnosis[24]-[26], ensuring efficient and precise results. Figure 1 illustrates the block diagram outlining the proposed methodology for precisely identifying fault location within the transformer core. Firstly, the

methodology involves extracting frequency components from a signal amidst noise and determining the amplitudes of the specific frequencies through Fourier transform. Secondly, machine learning algorithms are utilized to classify the fault location.

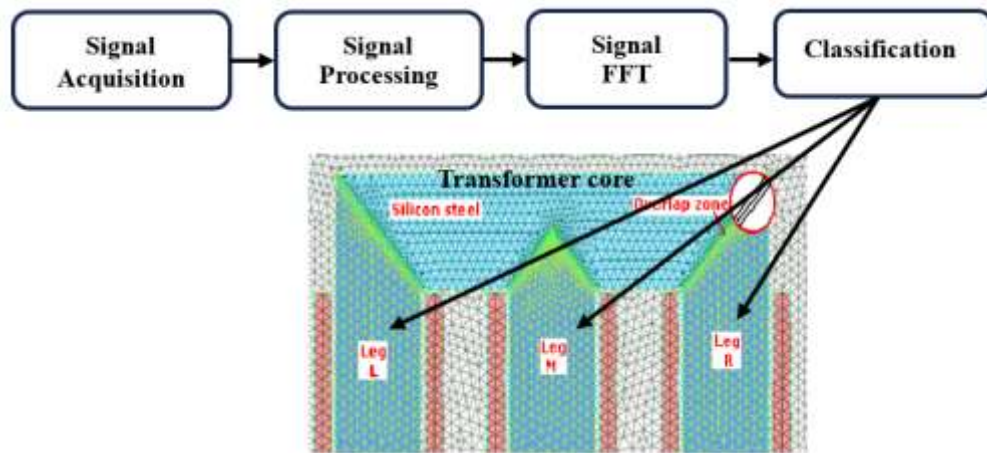


Figure 1. Proposed methodology

3. EXPERIMENTAL SETUP

In this particular investigation, a customized 2KVA-type transformer is being investigated. Table 1 presents the primary parameters that it possesses. There was a connection made between the output terminal of the transformer and a resistive load that could be adjusted at any power level between 0 and 100 kW. The accelerometer sensor 310A is integrated to the transformer with flat magnet mounting method. Sensor 310A with Digital USB signal conditioner was used for measuring vibration signals from test transformer tank surface under different load conditions. The sensitivity of 100 mV/g and the sampling frequency used to collect vibration signals was 12 KHz. To investigate the comprehensive vibration characteristics of the iron core, one measuring points have been positioned on the tank surface, as illustrated in Figure 2. These measurement locations have been carefully chosen to ensure proximity to the transformer core, which is securely fastened to the tank using bolts and nuts. In the testing process, the voltage regulator outputs the rated primary voltage, which is then applied to the transformer under examination. The load cabinet consists of a resistance cabinet; The load cabinet facilitates the adjustment of load magnitude. The platform can undergo testing under conditions of no-load, half load, and full load.

Table 1. 2KVA Power Transformer Details

S.L.	Categories	Parameter
1	Power Rating	2 KVA
2	High Voltage Rating	230V
3	Low Voltage Rating	115V
4	Operating Frequency	50Hz
5	Service conditions	Indoor

The E-I core being utilized in the construction of transformers may be seen in Figure 2(a). A total of three limbs and two yokes make up its core. In contrast to the other cores, the central limb comes with a double flux, which results in it having a breadth that is twice as wide. To understand the characteristics of a transformer with damaged core, intentionally deformed core sheet is inserted in the core legs (Leg Left, Leg Middle, Leg Right). This deformation may cause because of bending, torsion and twist in the transformer core limbs in out of plane direction. The core deformation occurs accidentally due to mechanical stresses or manufacturing defects. When a deformation is introduced in the core, it affects the inductance and reluctance of the transformer. With a deformation in the core, the inductance of the transformer decreases, and the reluctance increases. In high-current transformers, such as those used in power distribution or industrial applications, the changing magnetic field can induce significant physical stresses in the core. These stresses can result in the development of cracks over time. The cracks can further propagate due to the cyclic magnetic forces, leading to increased core losses and potential mechanical failure if not addressed. The experimental setup comprises a voltage regulator, an experimental transformer, and a load cabinet shown in Figure 2(b). The Figure 3 depicts the E shape core sheet with deformation in structure.

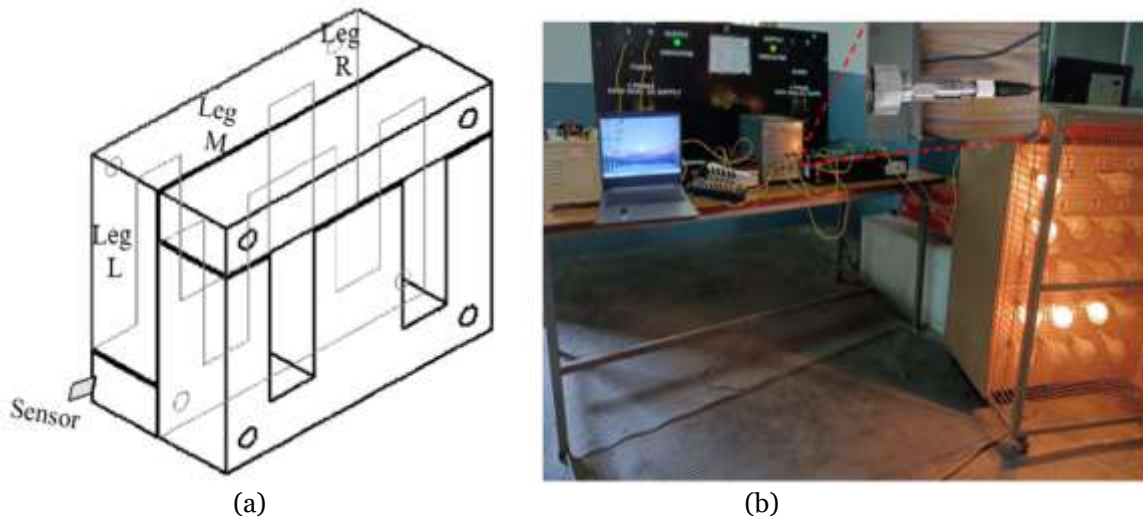


Figure 2. (a) EI shape transformer core (b) Transformer Testing Lab Setup

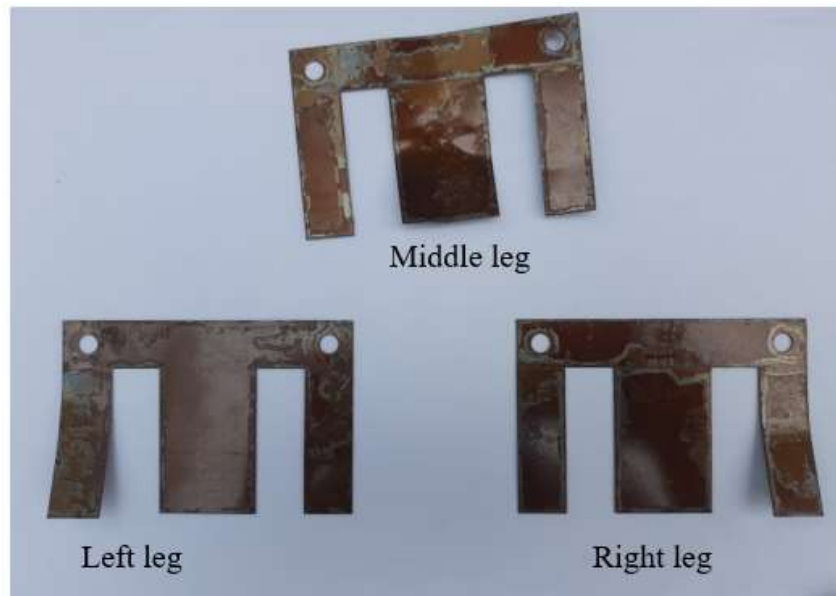


Figure 3. Deformed transformer core sheets

4. RESULTS AND DISCUSSION

To guarantee that the location of the core deformation, the vibrations is measured from the surface of the tank (as shown in Fig.2 (a)) appropriately represents the transformer internal behavior. The spectrum of vibration signals in time domain and frequency domain are studied as a criterion for determining the mechanical condition of the transformer core. Figure 4 shows the spectrum characteristics of vibration acceleration under full load healthy operating conditions. It is evident from the figure that in the case of a healthy core, the frequency spectrum is primarily concentrated around 100Hz.

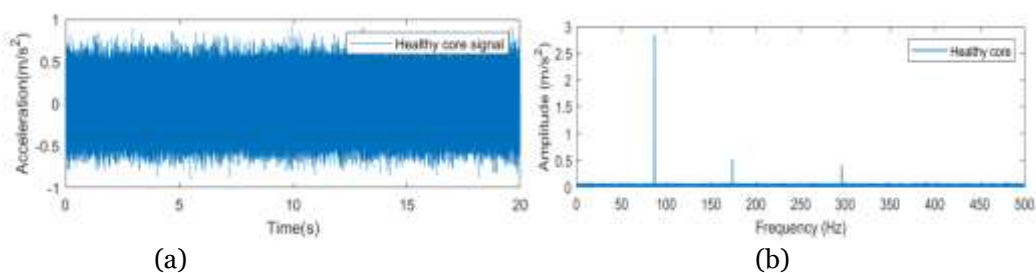


Figure 4. Vibrations of the Healthy transformer in the time and frequency domains.

Figure 5 shows a spectrum-analysis diagram of the vibration signals with a deformed core sheet inserted in the left leg, the amplitudes of vibration signals at frequencies of 100 Hz, 200 Hz and 300 Hz start to rise. This phenomenon occurs due to the presence of the deformation, which acts as an air gap, reducing the inductance and increasing the reluctance of the core. As a result, the deformation of the transformer core and the Lorentz force combine to amplify the vibration amplitudes at higher frequencies, such as 200 Hz, 300 Hz, and 400 Hz. Consequently, variations in core acceleration also led to changes in the noise emanating from the vicinity of the transformer.

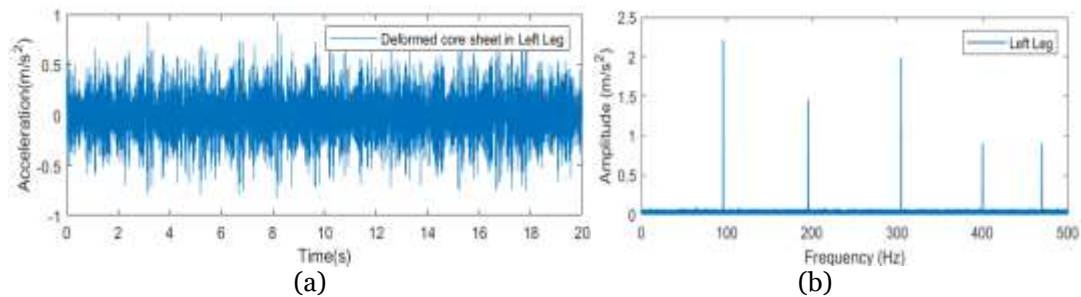


Figure 5 Vibrations of the transformer core with Left leg deformation in the time and frequency domains.

Figure 6 shows a spectrum-analysis diagram of the vibration signals with a deformed core sheet inserted in the middle leg, the amplitudes of vibration signals at frequencies of 100 Hz, 200 Hz and 300 Hz are reduced as compared to the left lag condition because from the measuring location machinal deformation point is shifted away.

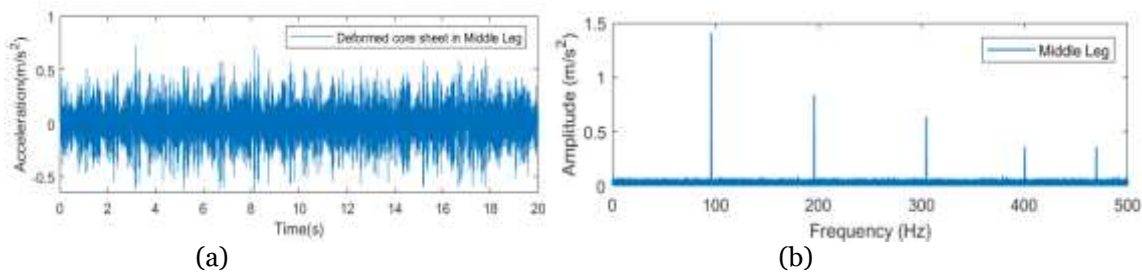


Figure 6 Vibrations of the transformer core with Middle leg deformation in the time and frequency domains.

Several machine learning algorithms, including gradient-based optimization methods, exhibit faster convergence when the input features share a similar scale. In cases where the features have significantly different scales, the algorithm might experience delayed convergence or even fail to converge.

Thus, collected vibration data is normalized between -1 and 1. Before commencing the model training, the dataset was partitioned into segments. Given that the data has a sampling frequency of 12 kHz, implying 12000 data samples per second, a single sample alone lacks adequate information about the vibration signal, including aspects such as amplitude, peak-to-peak value, behaviour, or frequency of one cycle. To address this limitation, a decision was made to consider 3000 samples, equivalent to 0.25 seconds of data, as one segment. This choice was made to encompass approximately four cycles of the vibration signal within each segment. By doing so, the intention is to provide the model with a more comprehensive view of the vibration data, enabling it to capture essential characteristics and patterns associated with input signal. This segmentation strategy aims to enhance the model's ability to discern meaningful features and relationships within the vibration data during the training process.

The CNN models employed for fault classification underwent training based on hyperparameters. Performance assessment during the training and validation processes was conducted by evaluating the classification accuracy. The model with the highest accuracy was identified and saved as the final model and it is shown in Figure 7. The final 1D-CNN structure encompasses five convolution layers, four pooling layers, and two fully connected layers. Primarily, the input data are the one-dimensional signal that has a length of 3000. First convolution layers use 128 convolution kernels of size 4×1 , second layer use 64 of size 4×1 third layer use 32 of size 4×1 layer, fourth layer use 16 of size 4×1 and fifth layer has 8 of size 4×1 . The output feature maps generated from convolution layers (layer 1 to 4) are fed into the max pooling layer as an input. Which carries out a 2×2 max-pooling operation. Within the flatten layer, the features extracted from the five convolution layers are expanded into a one-dimensional vector. The output layer comprises a four neuron. For this study, a softmax activation function is employed, representing classification post-training. The effectiveness of the proposed architecture for core fault classification is assessed through training and testing

processes. For this evaluation, 60% of the data is allocated to training, 20% for testing, and another 20% for validation.

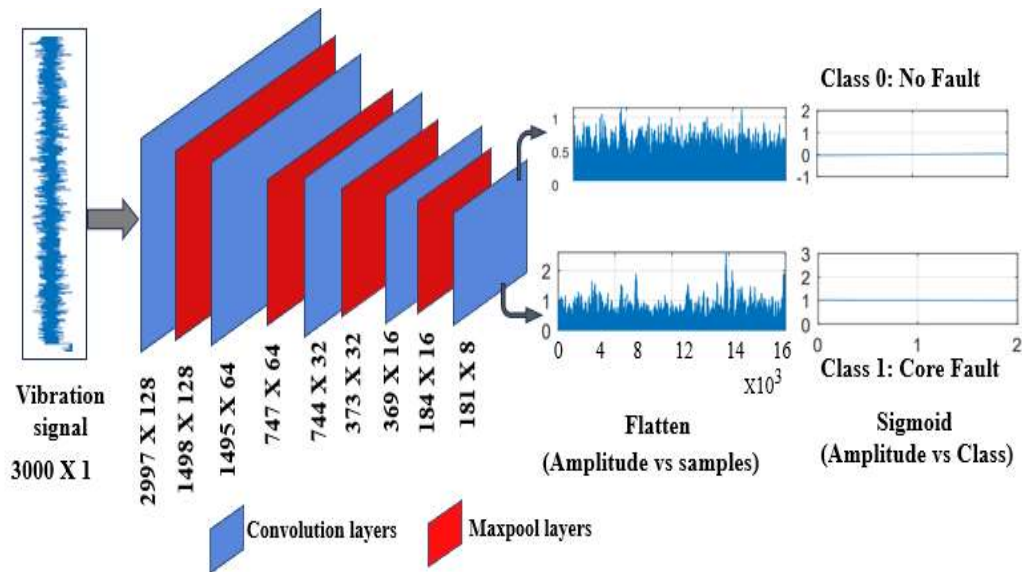


Figure 7 1D-CNN network structure for transformer core fault diagnosis[12].

A representation of the accuracy plot that corresponds to the number of iterations may be found in Figure 8. For the sake of this discussion, accuracy refers to the proportion of accurate predictions that the CNN model has produced. At first, while iterations are first being carried out, the accuracy is at a rather low level of roughly fifteen percent. In spite of this, there is a discernible rising trend that occurs as the iterations advance, culminating in a promising accuracy number of 96.33% at the conclusion of 400 iterations during the 40th epoch.

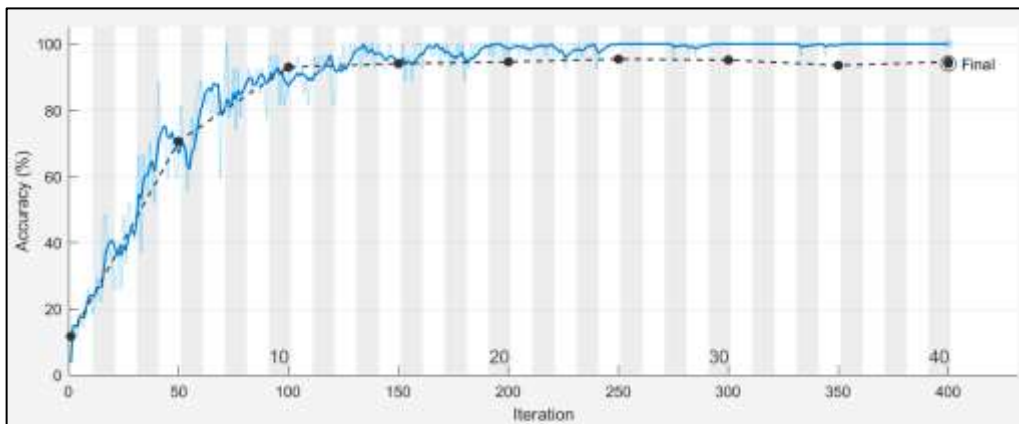


Figure 8. Accuracy and loss plot of the proposed CNN Model.

This rise in accuracy can be attributed to the CNN model being exposed to a greater number of scalogram images over the course of time, which ultimately results in classification that is more effective and exact. Figure 9 depicts the loss plot, which, in contrast to the accuracy plot, demonstrates an inverse relationship between the two. At first, the rate of loss is significantly higher than average, but it steadily decreases as the number of iterations (training) increases. This downward trend in loss is a natural outcome of the model's refinement and modification over the course of repeated iterations, which has resulted in more refined predictions and a reduction in mistakes.

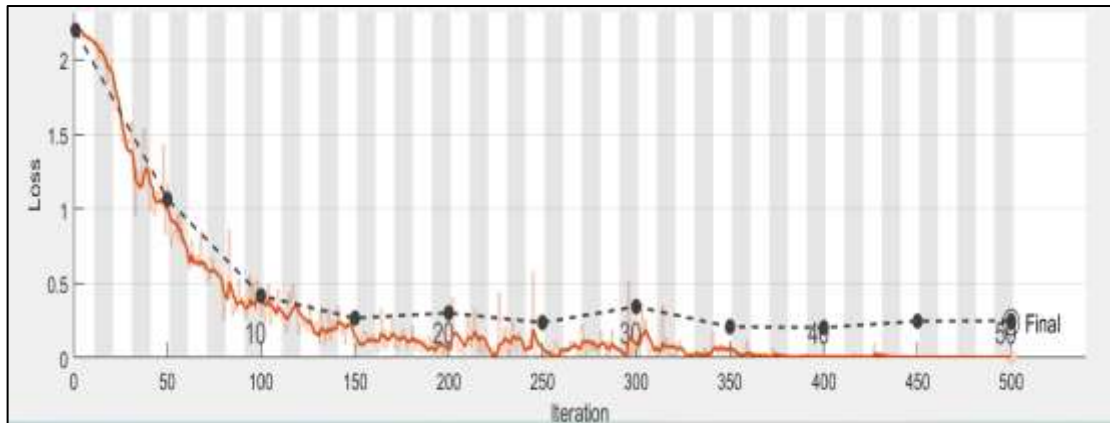


Figure 9. Loss plot of the proposed CNN Model.

The effectiveness of the proposed architecture for core fault classification is assessed through training and testing processes. For this evaluation, 60% of the data is allocated to training, 20% for testing, and another 20% for validation. Figures 8 illustrate the training curves, showcasing the progression of validation and training loss, as well as validation and training accuracy throughout the training epochs. The depicted curves indicate that the proposed architecture effectively learns from the provided data within a few epochs without overfitting. Ultimately, the achieved average classification accuracy for the proposed architecture is an impressive 99.78%. The comparative outcomes between the proposed methodology and existing works are presented in Table 2.

Table 2 Comparison table of related work

S.No	Reference	Year	Method	Accuracy%
1	[27]	2021	KNN	93.70
2	[28]	2019	SVM	94
3	[29]	2021	Fuzzy logic	93.85
4	[30]	2020	Fuzzy+RL	99.70
5	proposed	2024	CNN	99.78

Figure 10 is a representation of the confusion matrix that we have developed as a result of this scientific investigation. This is where we can observe the four classes, which include Leg L (deformation of the left leg), Leg M (deformation of the middle leg), and Leg R (deformation of the right leg as well). Within the Leg L class, 98 out of 100 instances have been successfully classified as Leg L. Similarly, within the Leg M and Leg R classes, 97 and 95 out of 100 cases have been successfully classified. There is a one hundred percent success rate for the Normal healthy class. Consequently, the overall average success percentage of the model that was utilized is currently at 96.6%.

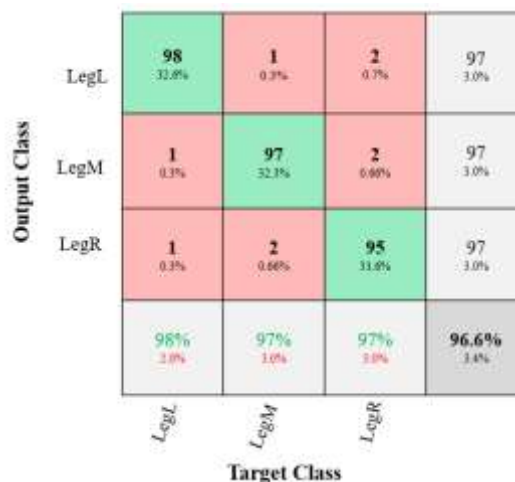


Figure 10. Confusion matrix for detection of the classes

5. CONCLUSION

This paper demonstrates the process of extracting features from measured data for condition monitoring and prognostics. These features are then utilized to develop dynamic models, which are subsequently validated and employed to predict the time of failures. This proactive approach allows for preemptive actions to be taken before actual failures occur. This paper presents an experimental investigation focused on the extraction of features from deformed transformer core. The study utilizes a 2 KVA transformer and examines the obtained results to explore the location of core deformation. Under normal conditions, the vibration frequency spectrum remains consistent at 100Hz and 200Hz, irrespective of the load current. However, in the presence of a deformed core, higher frequencies are observed alongside the changing load current and train a CNN neural network for classification purposes.

REFERENCES

- [1] C. Hunziker, J. Lehmann, T. Keller, T. Heim, and N. Schulz, "Sustainability assessment of novel transformer technologies in distribution grid applications," *Sustainable Energy, Grids and Networks*, vol. 21, Article ID 100314, 2020, <https://doi.org/10.1016/j.segan.2020.100314>.
- [2] Fan, J.; Shao, H.; Cao, Y.; Feng, L.; Chen, J.; Meng, A.; Yin, H. Condition Forecasting of a Power Transformer Based on an Online Monitor with EL-CSO-ANN. *Energies* **2022**, *15*, 8587. <https://doi.org/10.3390/en15228587>.
- [3] Y. C. Ma, J. Mo, G. Z. Wang et al., "Test and Experimental Study on vibration and noise characteristics of distribution transformer," *IOP Conference Series: Earth and Environmental Science*, vol. 526, Article ID 012136, 2020, <https://doi.org/10.1088/1755-1315/526/1/012136>.
- [4] F. Kabir, B. Foggo and N. Yu, "Data Driven Predictive Maintenance of Distribution Transformers," 2018 China International Conference on Electricity Distribution (CICED), Tianjin, China, 2018, pp. 312-316, doi: 10.1109/CICED.2018.8592417.
- [5] S. Pant, R. K. Nema and S. Gupta, "Detecting Faults in Power Transformers Using Wavelet Transform," 2021 IEEE 2nd International Conference On Electrical Power and Energy Systems (ICEPES), Bhopal, India, pp. 1-5, 2021.
- [6] Bicen, Propositional logic concept for fault diagnosis in complex systems. *Engineering Science and Technology, an International Journal*. Y. (2020), <https://doi.org/10.1016/j.jestch.2020.01.011>.
- [7] B.Pfützner, H. Relevance of magnetostriction and forces for the generation of audible noise of transformer cores. *IEEE Trans. Magn.* 2000, *36*, 3759–3777.
- [8] Smigiel Sandra & Pałczyński Krzysztof & Ledzinski Damian. (2021). ECG Signal Classification Using Deep Learning Techniques Based on the PTB-XL Dataset. *Entropy*. *23*. 1121. <https://doi.org/10.3390/e23091121> PMID: 34573746
- [9] Gupta Deepak & Khatri Bhavna & Dhiman Gaurav & Soni Mukesh & Gomathi S & Mane Dadaso. (2021). Review of ECG arrhythmia classification using deep neural network. *Materials Today: Proceedings*. <https://doi.org/10.1016/j.matpr.2021.05.249>.
- [10] Xiaoi Dai,¹Junying Cheng,¹Yu Gao,¹Shouheng Guo,¹Xingping Yang,¹Xiaoqian Xu,²and Yi Cen³ "Deep Belief Network for Feature Extraction of Urban Artificial Targets" 2387823, 1024-123X <https://doi.org/10.1155/2020/2387823>
- [11] Zhang, Y.; Liu, F. An Improved Deep Belief Network Prediction Model Based on Knowledge Transfer. *Future Internet* 2020, *12*, 188. <https://doi.org/10.3390/fi12110188>.
- [12] Nurmaini, S.; Darmawahyuni, A.; Sakti Mukti, A.N.; Rachmatullah, M.N.; Firdaus, F.; Tutuko, B. Deep Learning-Based Stacked Denoising and Autoencoder for ECG Heartbeat Classification. *Electronics* 2020, *9*, 135. <https://doi.org/10.3390/electronics9010135>.
- [13] Muhammad, Ghulam & Hossain, M. Shamim & Garg, Sahil. (2020). Stacked Autoencoder-Based Intrusion Detection System to Combat Financial Fraudulent. *IEEE Internet of Things Journal*. PP. 1-1. 10.1109/JIOT.2020.3041184.
- [14] R. Wang, Z. Li, J. Cao, T. Chen and L. Wang, "Convolutional Recurrent Neural Networks for Text Classification," 2019 International Joint Conference on Neural Networks (IJCNN), Budapest, Hungary, 2019, pp. 1-6, doi: 10.1109/IJCNN.2019.8852406.
- [15] Muhuri, P.S.; Chatterjee, P.; Yuan, X.; Roy, K.; Esterline, A. Using a Long Short-Term Memory Recurrent Neural Network (LSTM-RNN) to Classify Network Attacks. *Information* 2020, *11*, 243, <https://doi.org/10.3390/info11050243>.
- [16] He,¹² Q.; Fan, C.; Yang, G.; Li, H.; Li, J.; Chen, X. Experimental Analysis of Transformer Core Vibration and Noise under Inter-Harmonic Excitation. *Appl. Sci.* 2022, *12*, 1758, <https://doi.org/10.3390/app12031758>.
- [17] Fang, ¹³ Q.; Ye, Z.; Chen, C. A Review of Power Transformer Vibration and Noise Caused by Silicon Steel Magnetostriction. *Electronics*, *13*, 968, 2024, <https://doi.org/10.3390/electronics13050968>.
- [18] Qiang,¹⁴ He, Jingkai Nie, Songyang Zhang, Weimin, Xiao, Shengchang, Ji Xin, ChenPY. Study of Transformer Core Vibration and Noise Generation Mechanism Induced by Magnetostriction of Grain-Oriented Silicon Steel Sheet 8850780, 1070-9622, 2021, <https://doi.org/10.1155/2021/8850780>

- [19] Ramirez-Mendoza, Ricardo A., Qiang, He, Jingkai, Nie, Songyang, Zhang, Weimin, Xiao, "Study of Transformer Core Vibration and Noise Generation Mechanism Induced by Magnetostriction of Grain-Oriented Silicon Steel Sheet" 1070-9622 Hindawi, 2021, <https://doi.org/10.1155/2021/8850780>.
- [20] Xie, Y.; Chen, H.; Zhuang, Y.; Xie, Y. Fault Classification and Diagnosis Approach Using FFT-CNN for FPGA-Based CORDIC Processor. *Electronics* 2024, 13, 72. <https://doi.org/10.3390/electronics13010072>.
- [21] P. Agrawal et al., "YOLO Algorithm Implementation for Real Time Object Detection and Tracking," 2022 IEEE Students Conference on Engineering and Systems (SCES), Prayagraj, pp. 01-06, 2022, doi: 10.1109/SCES55490.2022.9887678.
- [22] Sahin, M.E., Ulutas, H., Yuca, E. et al. Detection and classification of COVID-19 by using faster R-CNN and mask R-CNN on CT images. *Neural Comput & Applic* 35, 13597–13611, 2023, <https://doi.org/10.1007/s00521-023-08450-y>.
- [23] Xiao, 20 Y.; Wang, X.; Zhang, P.; Meng, F.; Shao, F. Object Detection Based on Faster R-CNN Algorithm with Skip Pooling and Fusion of Contextual Information. *Sensors* 2020, <https://doi.org/10.3390/s20195490>
- [24] Li, C.; Chen, J.; Yang, C.; Yang, J.; Liu, Z.; Davari, P. Convolutional Neural Network-Based Transformer Fault Diagnosis Using Vibration Signals. *Sensors* 2023, 23, 4781, <https://doi.org/10.3390/s23104781>.
- [25] Priyanka Tiwari, Shweta Singh, Naresh B, Shirish Jain and Anand Goswami "1D-convolution neural network for transformer core fault identification" *International Journal of Applied Engineering & Technology*, Vol. 5 No.4, December, 2023.
- [26] Chen, C.-C.; Liu, Z.; Yang, G.; Wu, C.-C.; Ye, Q. An Improved Fault Diagnosis Using 1D-Convolutional Neural Network Model. *Electronics* 2021, 10, 59, <https://doi.org/10.3390/electronics10010059>
- [27] Kherif, O., Benmahamed, Y., Teguar, M., Boubakeur, A., and Ghoneim, S. S. M. (2021). Accuracy improvement of power transformer faults diagnostic using knn classifier with decision tree principle. *IEEE Access* 9, 81693–81701, 2021, 10.1109/ACCESS.2021.3086135.
- [28] Shang, H.; Xu, J.; Zheng, Z.; Qi, B.; Zhang, L. A Novel Fault Diagnosis Method for Power Transformer Based on Dissolved Gas Analysis Using Hypersphere Multiclass Support Vector Machine and Improved D–S Evidence Theory. *Energies* 2019, 12, 4017, <https://doi.org/10.3390/en12204017>
- [29] Poonnoy, N.; Suwanasri, C.; Suwanasri, T. Fuzzy Logic Approach to Dissolved Gas Analysis for Power Transformer Failure Index and Fault Identification. *Energies* 2021, <https://doi.org/10.3390/en14010036>.
- [30] Malik, H., Sharma, R., and Mishra, S. Fuzzy reinforcement learning based intelligent classifier for power transformer faults. *ISA Trans.* 101, 390–398. 2020, <https://doi.org/10.1016/j.isatra.2020.01.016>.